Role of Wingtip Substituents on Benzene-Platform-Based Tetrapodal Ligands toward the Formation of a Self-Assembled Silver Carbene Cage

B. Nisar Ahamed,[†] Ranjan Dutta, and Pradyut Ghosh*

Department of Inorganic Chemistry, Indian Association for the Cultivation of Science (IACS), 2A and 2B Raja S. C. Mullick Road, Kolkata 700032, India

Ⓢ *Supporting Information*
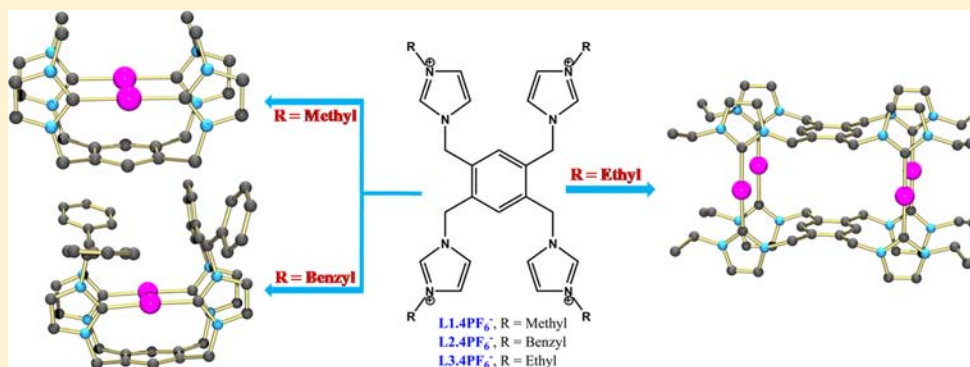
ABSTRACT: Tetrapodal imidazolium ligands L^1–L^3 as their PF_6^- salts are synthesized in good yields by reacting 1,2,4,5-tetrakis(bromomethyl)benzene with *N*-methylimidazole, *N*-benzylimidazole, and *N*-ethylimidazole, respectively. Single-crystal X-ray diffraction studies of $L^1 \cdot 4PF_6$, $L^2 \cdot 4PF_6$, and $L^3 \cdot 4PF_6$ show the chair conformation of the tetrapodal imidazoliums (L^1–L^3), where 1,5- and 2,4-imidazolium moieties are oriented in opposite directions of the benzene plane. The PF_6^- salts of L^1–L^3 are reacted with Ag_2O to synthesize different silver complexes of N-heterocyclic carbene (NHC), **1**–**3**, respectively, in good yields. Crystals of all three complexes suitable for single-crystal X-ray diffraction study are also isolated. Structural analysis of **1**, i.e., the complex of $L^1 \cdot 4PF_6$ containing methyl as a wingtip substituent, and Ag_2O shows the formation of a bimetallic silver NHC (NHC-Ag) complex, $[(L^1\text{-}4H)\cdot 2Ag]\cdot 2PF_6$, which is rotationally disordered over an inversion of symmetry of the space group $P2_1/c$. Elemental analysis and solution-state ^1H and ^{13}C NMR studies confirm the above molecular formula of complex **1**. When $L^2 \cdot 4PF_6$ functionalized with the benzyl wingtip moiety is explored for similar complexation with Ag_2O, the isolated complex **2** shows the formation of a simple NHC-Ag complex with molecular formula $[(L^2\text{-}4H)\cdot 2Ag]\cdot 2PF_6$, as observed in the case of **1**. Interestingly, the reaction of $L^3 \cdot 4PF_6$ containing ethyl as the wingtip substituent and Ag_2O shows the formation of a silver-ion-assisted tetranuclear molecular box of $[Ag_4(L^3\text{-}4H)_2]^{4+}$ (**3**).

■ INTRODUCTION

The construction of metal-ion-assisted supramolecular assemblies is a useful strategy to originate various interesting molecular architectures.[1] This has shown enormous current interest to the scientific community because of their aesthetically appealing topologies, potential applications in host–guest chemistry, and catalysis.[1,2] Many examples of such structurally fascinating compounds have been designed and synthesized via the assembly and preorganization of multidentate ligands based on accurate control of metal–ligand coordinate bond formation.[2] Many different varieties of molecular cages and cagelike discrete structures have been constructed using metallosupramolecular chemistry based on the coordination of nitrogen- and/or oxygen-donor atoms.[3] The self-assembly of metallosupramolecular structures via the formation of a metal–carbon (M–C) bond has been of increasing interest in the design and construction of a variety of supramolecular

topologies.[4] Recently, Hahn et al. have reported the construction of metallosupramolecular structures derived from the universal N-heterocyclic carbene (NHC) ligands using rigid tetra- and tripodal imidazolium receptors on a benzene platform.[4a,b] The steric and electronic properties of the substituents on the ligand and metal used for the construction of metallosupramolecular architectures are crucial for the self-assembly of the multipodal receptor via various supramolecular interactions and covalent bonds.[5] Although the formation of molecular cages with topologies like M_3L_2,[6a–c] M_4L_4,[6d] M_4L_6,[6e] M_6L_4,[6f] and M_6L_2[6g–k] (M = metal; L = ligand) is common in the literature, the formation of cages with M_4L_2 topology is rarely reported.[7] Similar to the reported flexible tetrapodal receptors on a benzene platform that form metallocages via

coordination of nitrogen with metal atoms, M—C bond formation may also lead to the isolation of various other elegant metallocages irrespective of the nature of the alkyl substituents.[4] In the case of M_4L_2 topology, the formation of metallocages arises upon coordination of metal ions via the dimeric assembly of planar rigid tetradendate receptors induced by twisting the planarity of the ligand system and M—C (NCN) bond formation. As a result, these planar tetradendate ligands mostly favor the formation of sandwich-shaped molecular cylinder architectures irrespective of the nature of the alkyl substituents. The ligand flexibility, steric hindrance, and coordinating mode of the metal atom increase the possibility of other products with different conformations. Significant advances in the variety of supramolecular metallocapsules have been made on the basis of planar rigid as well as flexible 1,3,5-substituted tripodal and 1,2,4,5-substituted tetrapodal receptors on a benzene platform via the coordination of nitrogen- and/or oxygen-donor atoms.[7] Recently, we have shown the formation of a hexanuclear metallocage by a benzene-based hexapodal receptor via the silver-ion-assisted dimeric assembly of the receptor.[6j] Herein, we demonstrate the effects of the wingtip substituents on ligands L^1–L^3 for the construction of metallosupramolecular architectures via M—C bond formation. We demonstrate the formation of a tetranuclear metallocage, $[Ag_4(L^3\text{-}4H)_2]^{4+}$ (i.e., **3**) via the silver-ion-assisted dimeric assembly of ethyl-substituted tetrapodal imidazolium receptor L^3. Further, we show the formation of binuclear silver NHC (NHC-Ag) complexes $[(L^1\text{-}4H)\cdot 2Ag]\cdot 2PF_6$ (**1**) and $[(L^2\text{-}4H)\cdot 2Ag]\cdot 2PF_6$ (**2**) in cases of tetrapodal receptors L^1 and L^2 having N-methyl and N-benzyl wingtips, respectively.

Designing Aspects. The proper choices of the framework and functionalities on the ligand are important toward the formation of metal-ion-assisted self-assembled supramolecular structures. Here our designing principles are as follows: (i) a new generation receptor with a 1,2,4,5-tetrasubstituted benzene moiety as our choice of framework for the formation of a M_4L_2 metallocage; (ii) variation in the wingtip substituents from methyl to benzyl and ethyl to understand their effect in the self-assembly process, if any; (iii) attachment of an N-alkylimidazolium ring via a benzylic spacer to the central benzene ring to impose a semirigid nature that can allow spatial segregation of arms around the central benzene ring; (iv) an N-alkylimidazolium ring chosen to act as a metal chelator via M—C bond formation; (v) the size and shape of the cage controlled by the relative orientation of the ligand and the geometry imposed by the metal ions; thus, Ag^+ is chosen to achieve a linear coordination geometry and to maximize the space between the ligands in metallocage formation.

■ EXPERIMENTAL SECTION

Materials and Methods. 1,2,4,5-Tetrakis(bromomethyl)benzene, N-methylimidazole, potassium hexafluorophosphate (KPF$_6$), and acetonitrile (CH$_3$CN) were purchased from Aldrich and were used directly without further purification. Silver oxide (Ag$_2$O), N-benzylimidazole, and diethyl ether were purchased from Cyanochem, India. Solvents were dried by conventional methods and distilled under a N$_2$ atmosphere before being used. N-Ethylimidazole was synthesized as per the literature procedures.[8]

Instrumentation. ^{1}H NMR measurements were recorded on Bruker 300 and 500 MHz FT-NMR spectrometers, and ^{13}C NMR spectra were recorded on Bruker 75 and 125 MHz FT-NMR spectrometers. Electrospray ionization (ESI) mass spectrometry measurements were carried out on a Qtof Micro YA263 high-resolution mass spectrometry (HRMS) instrument. Elemental analyses

for the ligands were carried out with a Perkin-Elmer 2500 series II elemental analyzer.

Crystallographic Refinement Details. The crystallographic data and details of data collection for ligands L^1–L^3 as their PF$_6^-$ salts and NHC complexes **1**–**3** are given in Tables 1 and 2, respectively. In each

Table 1. Crystallographic and Refinement Details of Tetrapodal Ligands L^1–L^3 as Their PF$_6^-$ Salts

parameter	$L^1\cdot 4PF_6$	$L^2\cdot 4PF_6$	$L^3\cdot 4PF_6$
empirical formula	$C_{26}H_{34}F_{24}N_8P_4$	$C_{50}H_{50}F_{24}N_8P_4$	$C_{30}H_{42}F_{24}N_8P_4$
fw	1038.49	1342.86	1094.60
cryst syst	orthorhombic	monoclinic	monoclinic
space group	$Pbca$	$P2_1/c$	$P2_1/n$
a (Å)	17.744(3)	7.3835(11)	10.2619(6)
b (Å)	9.3401(15)	30.819(5)	9.1305(6)
c (Å)	25.063(4)	12.4726(18)	23.0678(14)
α (deg)	90	90	90
β (deg)	90	91.070(4)	91.592(2)
γ (deg)	90	90	90
V (Å^3)	4153.7(12)	2837.7(7)	2160.5(2)
Z	4	2	2
d_{calcd} (g/cm^3)	1.661	1.572	1.683
crystal size (mm^3)	0.2 × 0.18 × 0.12	0.2 × 0.15 × 0.1	0.18 × 0.15 × 0.12
diffractometer	SMART CCD	SMART CCD	SMART CCD
$F(000)$	2088	1364.0	1108.0
μ(Mo Kα) (mm^{-1})	0.701	0.256	0.315
T (K)	150	150	150
θ_{max}	25	25.520	24.820
reflns collected	36600	27301	23874
indep reflns	3656	3538	3713
param refined	2498	389	301
R1, wR2	0.0784, 0.2715	0.0819, 0.2628	0.0502, 0.1303
GOF (F^2)	1.106	1.047	1.049

case, a crystal of suitable size was selected from the mother liquor, immersed in paratone oil, then mounted on the tip of a glass fiber, and cemented using epoxy resin. Intensity data for all six crystals were collected using Mo Kα radiation (λ = 0.7107 Å) on a Bruker SMART APEX diffractometer equipped with a CCD area detector at 150 K. Data integration and reduction were processed with *SAINT* software.[9a] An empirical absorption correction was applied to the collected reflections with *SADABS*.[9b] Structures were solved by direct methods using *SHELXTL*[10] and were refined on F^2 by a full-matrix least-squares technique using the *SHELXL-97* program package.[11] Graphics were generated using *PLATON*[12] and *MERCURY 2.3*.[13] In all cases, non-hydrogen atoms were treated anisotropically and all of the hydrogen atoms attached with carbon atoms were geometrically fixed. Further, to understand the rotational disorder of the complex around inversion symmetry in the crystal structure of **1**, we have refined the crystal structure by keeping the site occupancy factor (SOF) = 0.5 for the carbon atom of the benzene platform and 1 for the rest of atoms. In complex **3**, from the difference Fourier map, a number of diffused scattered peaks with electron density were observed, which can be attributed to the disordered solvent present in this complex. Attempts to model these peaks were unsuccessful because the residual electron density peaks obtained were diffused. *PLATON/SQUEEZE*[12] was used to refine the structure further. Total potential solvent-accessible area volumes of 702.5 Å^3 and 292 electron counts/unit cell were found. This electron count corresponds tentatively to four diethyl ether molecules present in the unit cell. Thus, the structure of complex **3** revealed four lattice diethyl ether molecules in the asymmetric unit in the lattice, whose contribution is removed by the *PLATON/SQUEEZE* program.

Table 2. Crystallographic and Refinement Details of Complexes 1−3

parameter	1, $Ag_2(L^1$-4H)·2PF$_6$	2, $Ag_2(L^2$-4H)·2PF$_6$	3, $Ag_4(L^3$-4H)$_2$·4PF$_6$
empirical formula	$C_{13}H_{13}AgF_6N_4P$	$C_{54}H_{46}Ag_2F_{12}N_8OP_2$	$C_{60}H_{76}Ag_4F_{24}N_{16}P_4$
fw	478.11	1328.67	2032.73
cryst syst	monoclinic	monoclinic	tetragonal
space group	$P2_1/c$	$P2_1/n$	$P4_2/mnm$
a (Å)	8.9599(5)	11.722(4)	18.3487(18)
b (Å)	12.4841(7)	22.308(7)	18.3847(18)
c (Å)	14.9233(8)	21.567(7)	13.0310(14)
α (deg)	90.00	90	90
β (deg)	91.400(2)	97.334(9)	90
γ (deg)	90.00	90	90
V (Å^3)	1668.77(16)	5594(3)	4387.2(8)
Z	4	4	2
d_{calcd} (g/cm^3)	2.050	1.578	1.539
cryst size (mm^3)	0.20 × 0.1 × 0.08	0.1 × 0.05 × 0.01	0.2 × 0.10 × 0.08
diffractometer	SMART CCD	SMART CCD	SMART CCD
$F(000)$	940.0	2664.0	2024.0
μ(Mo Kα) (mm^{-1})	1.370	0.844	1.047
T (K)	150	150	150
θ_{max}	24.730	19.090	24.990
reflns collected	18831	35635	9805
indep reflns	2846	4550	2128
param refined	253	712	1962
R1, wR2	0.0587, 0.2118	0.0485, 0.1236	0.0334, 0.1221
GOF (F^2)	0.951	1.052	1.098

Synthesis of L^1·4PF$_6$. 1,2,4,5-Tetrakis(bromomethyl)benzene (0.450 g, 1 mmol) was dissolved in 50 mL of dry CH$_3$CN under a N$_2$ atmosphere. *N*-Methylimidazole (0.410 g, 5 mmol) was added to the reaction mixture under a N$_2$ atmosphere with constant stirring and was refluxed overnight. A white precipitate was formed. Then the temperature of the reaction was gradually brought to room temperature, and the white solid was filtered and washed with CH$_3$CN to remove excess *N*-methylimidazole. The residue was dissolved in 50 mL of water, and then a saturated solution of KPF$_6$ was added with constant stirring for 1 h. Then white precipitate was filtered and washed with water and allowed to dry in air. Yield: 76%. ^{1}H NMR (500 MHz, DMSO-d_6): δ 7.52 (s, 4H, NCHN), 6.27 (s, 4H, imida CH), 6.05 (s, 4H, imida CH), 5.71 (s, 2H, phenyl CH), 4.03 (s, 8H, benzyl CH$_2$), 2.37 (s, 12H, methyl CH$_3$). ^{13}C NMR (125.8 MHz, DMSO-d_6): δ 36.51, 49.04, 122.80, 124.64, 131.98, 134.67, 137.42. HRMS (ESI). Calcd for $[L^1 + 3PF_6]^+$: m/z 893.1810. Found: m/z 893.1165. Anal. Calcd for $C_{26}H_{34}F_{24}N_8P_4$: C, 30.07; H, 3.30; N, 10.79. Found: C, 30.16; H, 3.39; N, 10.61.

Synthesis of L^2·4PF$_6$ and L^3·4PF$_6$. Two other tetrapodal imidazolium ligands, L^2·4PF$_6$ and L^3·4PF$_6$, were prepared following the procedure adopted in the case of L^1·4PF$_6$, where *N*-benzylimidazole and *N*-ethylimidazole were used, respectively, instead of *N*-methylimidazole.

L^2·4PF$_6$. Yield: 72%. ^{1}H NMR (500 MHz, DMSO-d_6): δ 9.11 (s, 4H, NCHN), 7.81 (s, 4H, imida CH), 7.52 (s, 4H, imida CH), 7.40−7.34 (m, 20H, phenyl CH), 5.56 (s, 8H, benzyl CH$_2$), 5.37 (s, 8H, benzyl CH$_2$), 5.58 (s, 8H, benzyl CH$_2$). ^{13}C NMR (125.8 MHz, DMSO-d_6): δ 16.81, 48.33, 52.66, 123.03, 123.37, 128.61, 129.35, 129.58, 130.00, 135.36, 136.52, 141.69. HRMS (ESI). Calcd for $[L^2 + 3PF_6 − 2H]^+$: m/z 1195.3062. Found: m/z 1195.0889. Anal. Calcd for $C_{50}H_{50}F_{24}N_8P_4$: C, 44.72; H, 3.75; N, 8.34. Found: C, 44.39; H, 3.55; N, 8.22.

L^3·4PF$_6$. Yield: 78%. ^{1}H NMR (500 MHz, DMSO-d_6): δ 8.86 (s, 4H, NCHN), 7.82 (s, 4H, imida CH), 7.30 (s, 4H, imida CH), 5.58 (s, 8H, benzyl CH$_2$), 4.18 (t, 8H, ethyl CH$_2$), 1.41 (t, 12H, methyl CH$_3$). ^{13}C NMR (125.8 MHz, DMSO-d_6): δ 15.04, 44.56, 46.77, 121.88, 122.01, 135.69, 137.99. HRMS (ESI). Calcd for $[L^3 + 3PF_6]^+$: m/z 949.2436. Found: m/z 949.5740. Anal. Calcd for $C_{30}H_{42}F_{24}N_8P_4$: C, 32.92; H, 3.87; N, 10.24. Found: C, 33.05; H, 3.72; N, 10.11.

Synthesis of Complex 1. A sample of L^1·4PF$_6$ (0.089 g, 0.1 mmol) was dissolved in 5 mL of CH$_3$CN, and Ag$_2$O (0.049 g, 0.21 mmol) was added to this solution. Then the resulting mixture was heated to 70 °C for 24 h under dark conditions. The final suspension was filtered after cooling to ambient temperature. The filtrate was concentrated to 2 mL, and then 10 mL of diethyl ether was added to the concentrated filtrate, which led to the formation of a white microcrystalline solid. The solid was collected by filtration, washed with diethyl ether, and dried in vacuo. Single crystals suitable for X-ray structural analysis of complex **1** were obtained either by the slow vapor diffusion of diethyl ether to a saturated CH$_3$CN solution of the crude product or by the slow evaporation of a CH$_3$CN solution of the crude product. Yield: 70%. ^{1}H NMR (500 MHz, CD$_3$CN): δ 7.96 (s, 4H, aryl CH), 7.02 (s, 4H, imida CH), 6.80 (s, 4H, imida CH), 5.59 (d, 4H, benzyl CH), 5.14 (d, 4H, benzyl CH), 3.59 (s, 12H, methyl). ^{13}C NMR (125.8 MHz, CD$_3$CN): δ 39.54, 51.52, 121.43, 123.51, 136.09, 140.09. HRMS (ESI). Calcd for $[L^1 + 2Ag + 3PF_6 − 5H]^-$: m/z 1104.9617. Found: m/z 1105.7960. Anal. Calcd for $C_{26}H_{34}Ag_2F_{12}N_8P_2$: C, 32.39; H, 3.55; N, 11.62. Found: C, 32.33; H, 3.61; N, 11.45.

Synthesis of Complexes 2 and 3. Complexes **2** and **3** were prepared using L^2·4PF$_6$ and L^3·4PF$_6$, respectively, following the procedure adopted in the case of complex **1**.

2. Yield: 64%. ^{1}H NMR (500 MHz, DMSO-d_6): δ 7.25− 6.973 (m, 28H), 5.35 (b, 8H, benzyl CH$_2$−), 5.11 (s, 8H, benzyl CH$_2$). ^{13}C NMR (125.8 MHz, DMSO-d_6): δ 136.69, 135.84, 129.00, 128.36, 127.41, 124.15, 121.04, 56.24, 51.75, 21.62. Anal. Calcd for $C_{54}H_{60}Ag_2F_{12}N_8OP_2$: C, 48.30; H, 4.50; N, 8.34. Found: C, 48.37; H, 4.58; N, 8.45. Complex **2** is highly photosensitive in nature; upon exposure to light, its color changes from colorless to black. No satisfactory data are obtained in mass spectral data analysis.

3. Yield: 68%. ^{1}H NMR (500 MHz, DMSO-d_6): δ 8.20 (s, 2H, aryl CH), 7.27 (s, 4H, imida CH), 7.15 (s, 4H, imida CH), 5.87 (d, 4H, benzyl CH), 5.82 (d, 4H, benzyl CH), 3.88 (q, 8H, NCH$_2$CH$_3$), 1.23 (t, 12H, NCH$_2$CH$_3$). ^{13}C NMR (125.8 MHz, DMSO-d_6): δ 139.33, 135.79, 123.43, 119.93, 50.83, 47.41, 16.89. HRMS (ESI). Calcd for $[L^3 + 2Ag + 3PF_6 + 2Na + Cl − 5H]^-$: m/z 1240.9727. Found: m/z 1240.0367. Anal. Calcd for $C_{60}H_{76}Ag_4F_{24}N_{16}P_4$: C, 35.45; H, 3.77; N, 11.03. Found: C, 35.51; H, 3.80; N, 11.11.

■ RESULTS AND DISCUSSION

Synthesis. Tetrapodal receptors (L^1–L^3) as their PF_6^- salts are synthesized in good yields upon reaction of 1,2,4,5-tetrakis(bromomethyl)benzene with *N*-methylimidazole, *N*-benzylimidazole, and *N*-ethylimidazole, respectively, and in situ exchange of an anion from Br^- to PF_6^-, as shown in Scheme 1. Single crystals of L^1–L^3 with PF_6^- counteranions are

Scheme 1. General Schematic Diagram for the Syntheses of Tetrapodal Receptors L^1–L^3 as PF_6^- Salts

$L^1 \cdot 4PF_6$, R_1- CH_3
$L^2 \cdot 4PF_6$, R_1- Benzyl
$L^3 \cdot 4PF_6$, R_1- CH_2CH_3
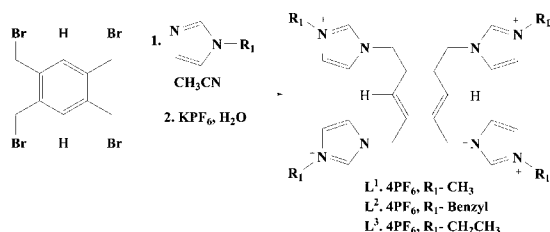
also isolated in good yields upon the slow evaporation of their saturated CH_3CN solution. The crystallographic details of these receptors are listed in Table 1. Ligands $L^1 \cdot 4PF_6$, $L^2 \cdot 4PF_6$, and $L^3 \cdot 4PF_6$ are crystallized in orthorhombic (*Pbca*), monoclinic (*P2$_1$/c*), and monoclinic (*P2$_1$/n*) space groups, respectively. The single-crystal X-ray structures of the PF_6^- salts of L^1–L^3 show chair conformation where 1,5-imidazolium moieties are on one side and 2,4-imidazolium moieties are oriented on the opposite side of the benzene plane (Figure 1). In $L^1 \cdot 4PF_6$, all of the acidic protons of the imidazolium rings are located in an inward direction toward the clefts and hydrogen-bonded with PF_6^- via C−H⋯F interactions with bond distances of F2⋯C2 = 3.428 Å, F4A⋯C2 = 3.206 Å, F4B⋯C2 = 3.245 Å, F4B⋯C10 = 3.144 Å, F4⋯C10 = 3.108 Å, F10⋯C8 = 3.311 Å, F5⋯C13 = 3.413 Å, F8⋯C12 = 3.339 Å, and F7⋯C11 = 3.251 Å, as shown in the Supporting Information (SI; Figure S19). $L^2 \cdot 4PF_6$ shows the orientation of one imidazolium ring toward the inner cavity, and the other is in an outward direction among two acidic protons of imidazolium rings that are on one side of the benzene plane. Binding of PF_6^- in the cavity of L^2 occurred via acidic imidazolium C−H⋯F interaction of one arm and aryl C−H⋯F interaction of another arm with bond distances of C6⋯F1 = 3.072 Å and C16⋯F1 = 3.174 Å, as shown in the SI (Figure S20). The outward-oriented acidic imidazolium CH, phenyl CH, and benzyl CH_2 are making room for the binding

of PF_6^- in the cleft of the tetrapodal receptor L^2 via C−H⋯F interactions with bond distances of C11⋯F8 = 3.564 Å, C1⋯F12 = 3.410 Å, and C18⋯F12 = 3.054 Å, as shown in Figure S20 (SI). Crystal structure analysis of $L^3 \cdot 4PF_6$ shows an orientation of acidic protons of imidazolium arms similar to that observed in $L^1 \cdot 4PF_6$.

Two of the PF_6^- anions are located in the cavity via C−H⋯F interactions with bond distances of C12⋯F1 = 3.253 Å, C3⋯F1 = 3.179 Å, and C13⋯F3 = 3.378 Å, whereas the remaining two PF_6^- anions are found in the cleft via C−H⋯F interactions with bond distances of C15⋯F11 = 3.257 Å and C9⋯F9 = 3.313 Å (SI, Figure S21). The cleft binding of PF_6^- in $L^3 \cdot 4PF_6$ is further strengthened with the binding of an acidic imidazolium moiety via C−H⋯F interactions with a bond distance of C12⋯F10 = 2.871 Å and via ethyl C−H⋯F interactions with a bond distance of C1⋯F10 = 3.597 Å (SI, Figure S21).

Complex 1. Complexation of $L^1 \cdot 4PF_6$ having methyl as the wingtip on a benzene platform with Ag_2O has been carried out at 70 °C for 24 h in CH_3CN (Scheme 2). The single crystals of

Scheme 2. Reaction of L^1 with Ag_2O in CH_3CN
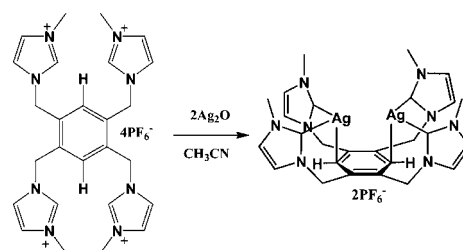
a L^1-NHC-Ag complex (i.e., **1**) are obtained upon the slow evaporation of a CH_3CN solution or by a diethyl ether diffusion technique. A single-crystal X-ray diffraction study shows that complex **1** crystallizes in the centrosymmetric monoclinic space group *P2$_1$/c*. The asymmetric unit contains an unexpected macrocycle, wherein one Ag^+ is coordinated by the imidazole carbon atoms. Growing the asymmetric unit further by applying crystallographic space group symmetry resulted in an unusual bimetallic complex with a cage structure (SI, Figure S22). Further investigation revealed that the C−C bond distances involving the methylene moieties attached to the imidazole rings are unusually large (C5−C4 = 1.665 Å, C7−C8 = 1.53 Å, C13−C12 = 1.717 Å, and C15−C16 = 1.664 Å). Crystallo-
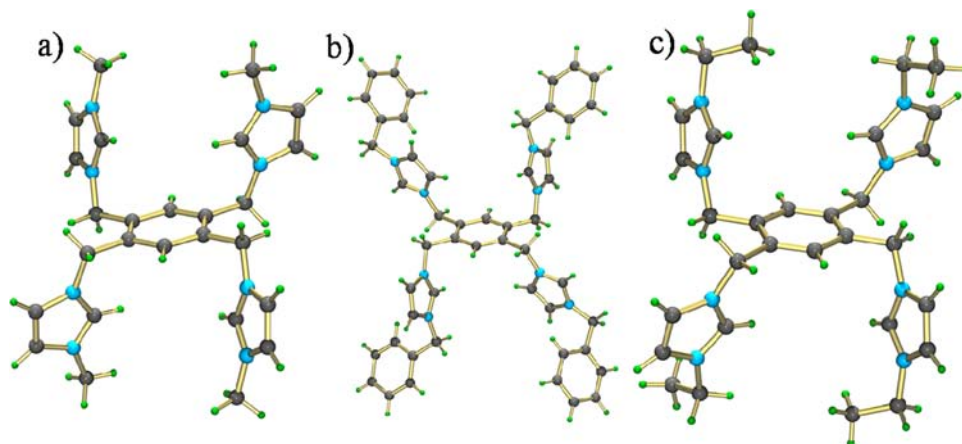
Figure 1. Single-crystal X-ray structure of compounds (a) L^1, (b) L^2, and (c) L^3 (PF_6^- anions are removed for clarity).

graphic refinement, keeping SOF = 1.0 for all of the located atoms, results in high thermal parameters for most of the atoms with a final R factor of 7.3%. However, elemental analysis and solution-state ^{1}H and ^{13}C NMR studies of the crystals indicated the formation of a NHC-Ag complex having a composition of $[(\mathbf{L^1}\text{-4H})\cdot 2\text{Ag}]\cdot 2\text{PF}_6$. Thus, we have examined the X-ray data further and realized that it is indeed a bimetallic NHC-Ag complex $[(\mathbf{L^1}\text{-4H})\cdot 2\text{Ag}]\cdot 2\text{PF}_6$, which is rotationally disordered over a center of symmetry of the space group $P2_1/c$. Final refinement, keeping SOF = 1.0 for imidazole moieties, Ag$^+$ and PF$_6$, and 0.5 for the other six carbon atoms of the central arene, gave an R factor of 5.9% with improved thermal parameters of most of the atoms. Figure 2 depicts the single-crystal X-ray
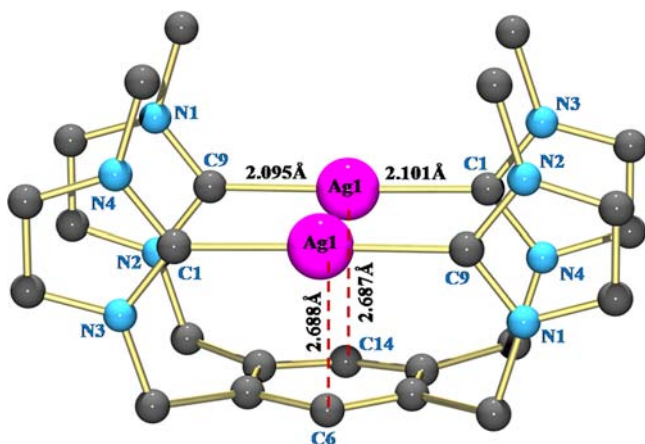
Figure 2. Perspective view of the $[(\mathbf{L^1}\text{-4H})\cdot 2\text{Ag}]$ NHC complex **1** (PF$_6^-$ anions are omitted for clarity).

structure of bimetallic NHC complex **1**, $[(\mathbf{L^1}\text{-4H})\cdot 2\text{Ag}]\cdot 2\text{PF}_6$. The detailed crystal structure analysis of **1** shows that the silver atoms are in a T-shaped geometry (Figure 2). The silver atoms are coordinated with two of the alternate imidazolium carbon atoms (NCN) with bond distances of Ag1−C1 = 2.101(9) Å and Ag1−C9 = 2.095(9) Å and a bond angle of ∠C1−Ag1−C9 = 177.01(3)°. Further, the silver atoms exhibit strong metal− arene interaction with bond distances of Ag1−C6 = 2.688(12) Å and Ag1−C14 = 2.687(14) Å and bond angles of ∠C7−C6− Ag1 = 88.64(7)° and ∠Ag1−C6−C5 = 87.1(7)°. The distance between the two imidazolium rings is Cg3−Cg4 = 3.536 Å. The bond distance between the two silver atoms is 3.359 Å, which is slightly less than the sum of the van der Waals radii of two silver atoms (3.44 Å).
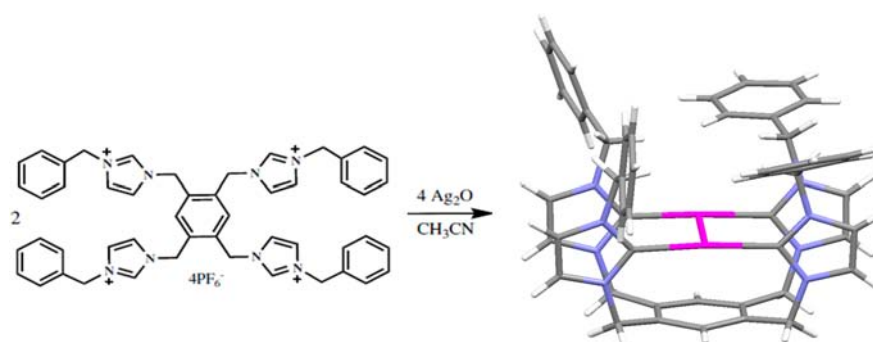
Solution-State ^{1}H and ^{13}C NMR Analysis of Crystals of 1.

^{1}H NMR analysis of the single crystals of **1** in the solution state shows a singlet at 3.60 ppm, which is ascribed to the methyl protons of the N-methylimidazole functionality, and two doublets at 5.15 and 5.60 ppm, which are assigned as benzylic protons (SI, Figure S10). In contrast, $\mathbf{L^1}\cdot 4\text{PF}_6$ shows a sharp singlet at 4.03 ppm corresponding to the benzylic protons. These suggest the existence of the NHC-Ag complex $[(\mathbf{L^1}\text{-4H})\cdot 2\text{Ag}]\cdot 2\text{PF}_6$, as shown in Scheme 2 and Figure 2. Further, the existence of metal−arene interaction between the silver atoms with the aryl moiety in $\mathbf{L^1}\cdot 4\text{PF}_6$ in the solution state is also established from the ^{13}C NMR study. The ^{13}C NMR spectrum of **1** shows a ∼8.13 ppm downfield shift of an aryl carbon functionalized with the benzyl moiety (aryl *C*CH$_2$, 140.11 ppm) compared to that of $\mathbf{L^1}\cdot 4\text{PF}_6$ (aryl *C*CH$_2$, 131.98 ppm). On the other hand, the aryl CH in **1** appears in the downfield region at 136.59 ppm compared to $\mathbf{L^1}\cdot 4\text{PF}_6$ (aryl CH, 134.67 ppm; SI, Figure S2). These suggest the existence of metal−arene interaction between the silver atoms with the aryl moiety of **1** in the solution state similar to that observed in the solid-state structural analysis of **1**. Further elemental analysis of the crystals confirmed that the composition of the NHC-Ag complex of **1** is $[(\mathbf{L^1}\text{-4H})\cdot 2\text{Ag}]\cdot 2\text{PF}_6$.

Complex 2. To overcome rotational disorder over an inversion of symmetry of the space group $P2_1/c$, as observed in the case of **1**, we have synthesized the tetrapodal receptor $\mathbf{L^2}\cdot 4\text{PF}_6$ by changing the wingtip substituent from methyl to the benzyl moiety. The reaction of $\mathbf{L^2}\cdot 4\text{PF}_6$ with Ag$_2$O has been carried out in CH$_3$CN, as shown in Scheme 3.

Single crystals of the NHC complex **2** are obtained upon the slow vapor diffusion of diethyl ether to a saturated solution of the reaction mixture in the dark. The quality of the crystals obtained is poor, and we could not improve the quality even after repeated attempts of crystallization. Further, this crystal has a tendency to turn black in the presence of light. With extreme care, we were able to collect the data of complex **2**. Crystal structure analysis of complex **2** suggests the existence of a simple $[(\mathbf{L^2}\text{-4H})\cdot 2\text{Ag}]\cdot 2\text{PF}_6$ complex, similar to the $[(\mathbf{L^1}\text{-4H})\cdot 2\text{Ag}]\cdot 2\text{PF}_6$ complex. In this case, deprotonation of the CH protons at the acidic carbon atoms of $\mathbf{L^2}\cdot 4\text{PF}_6$ led to the formation of the NHC-Ag complex **2**, in which all of the tetrapodal arms are oriented in one direction with the formation of a Ag−C (NCN) bond, as observed in complex **1** (Figure 3).

The silver atom is linearly bonded between two of the carbon atoms of alternate imidazolium rings with bond distances of Ag1−C13 = 2.103(11) Å, Ag1−C16 = 2.091(11) Å and Ag2− C14 = 2.098(11) Å, Ag2−C15 = 2.094(11) Å and with bond

Scheme 3. Reaction of L^2·4PF$_6$ with Ag$_2$O in CH$_3$CN
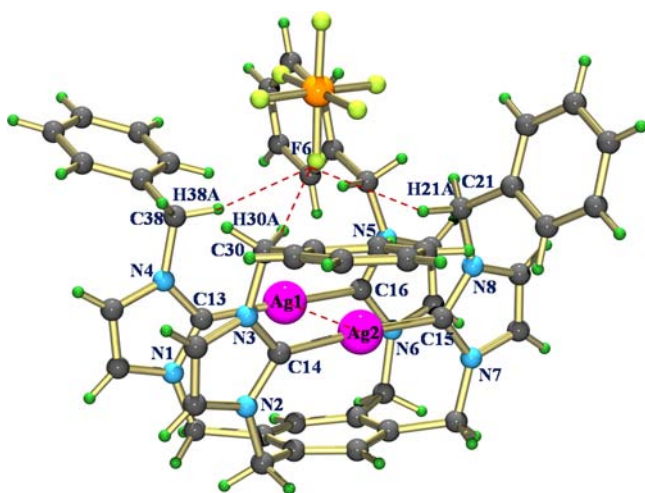
Figure 3. Perspective view of the $L^2 \cdot 4PF_6$ NHC-Ag complex **2**. The PF_6^- anions are omitted for clarity.

Figure 4. Perspective view of the $[Ag_4(L^3\text{-}4H)_2]^{4+}$ molecular box (PF_6^- anions are omitted for clarity).

angles of $\angle$C13−Ag1−C16 = 173.5(4)° and $\angle$C14−Ag2−C15 = 176.0(5)°. The benzyl moieties of complex **2** are making a pocket in which one of the counteranions PF_6^- is in C−H···F interaction with bond distances of C30···F6 = 3.492 Å, C38···F6 = 3.384 Å, and C21···F6 = 3.321 Å. The Ag−Ag bond distance in complex **2** is about 0.2 Å less than the sum of their van der Waals radii [Ag1−Ag2 = 3.215(15) Å]. In this complex, there is no such metal−arene interaction as that observed in the case of complex **1**.

Complex 3. To understand the role of the wingtip substituent, we have further synthesized the tetrapodal receptor $L^3 \cdot 4PF_6$ with an ethyl moiety for complexation with Ag_2O, as shown in Scheme 4. The reaction of $L^3 \cdot 4PF_6$ with Ag_2O in CH_3CN leads to the formation of the NHC-Ag complex **3**. The crystals of **3** are obtained upon the slow evaporation of the reaction mixture in the dark. Interestingly, single-crystal X-ray structural analysis shows the formation of a molecular box, $[Ag_4(L^3\text{-}4H)_2] \cdot 4PF_6$, via the formation of a NHC−Ag bond and the dimeric self-assembly of L^3 (Figure 4). The chair conformation of L^3 is now oriented unidirectionally in complex **3**, where all of the imidazolium moieties are on one side of the benzene plane (Scheme 4). Deprotonation at the acidic C−H bond of carbon atoms (NCN) by Ag_2O in $L^3 \cdot 4PF_6$ leads to orientation of all of the tetrapodal arms of $L^3 \cdot 4PF_6$ on one side via the formation of Ag−C bonds. The coordination of four Ag^+ ions with the four acidic carbon atoms of another molecule of L^3 results in a $[Ag_4(L^3\text{-}4H)_2]^{4+}$ molecular box, **3**, with a Ag1−C1 bond distance of 2.091(4) Å (Figure 4). In the molecular box, the distance between the two centroids of the apical benzene rings Cg1−Cg2 is 4.923 Å. In the box, all imidazolium rings are oriented orthogonal to the benzene rings with a centroid distance between the two imidazolium rings Cg3−Cg4 of 4.481 Å. The distance between the two silver atoms Ag1−Ag1 in complex **3** is found to be 4.938 Å.

■ CONCLUSION

In conclusion, we have developed three tetrapodal hosts with different wingtip-substituted ligands for the silver-ion-assisted construction of metallosupramolecular architectures via M−C bond formation. Short Ag−C−H interactions[14] between the aryl carbon atoms and the metal center have been observed in the case of **1**, where the ligand contains a methyl wingtip substituent. Complex of $L^2 \cdot 4PF_6$ having a benzyl wingtip substituent and Ag_2O, i.e., **2**, shows the formation of a similar silver complex of NHC such as that of **1**; however, in this case, no such metal−arene interaction is observed as in the case of **1**. In complex **2**, metal−metal interaction has been established from shorter Ag−Ag distances in the single-crystal X-ray study. Complex **3** obtained from $L^3 \cdot 4PF_6$ having ethyl as the wingtip substituent forms silver-ion-assisted metallocage **3** via dimeric assembly of the ligands. This demonstrates that upon tuning of the wingtip substitution of the tetrapodal imidazolium ligands different supramolecular interactions, such as metal−arene interaction, metal−metal interaction, and self-assembled structure formation, can be achieved, during complexation with Ag_2O. We believe that the tuning of wingtip substitution on the receptor for the construction of metallosupramolecular architectures via M−C bond formation in the present study has great importance in the construction of various metallocages for host−guest chemistry.

Scheme 4. Formation of a Molecular Box by the Reaction of $L^3 \cdot 4PF_6$ with Ag_2O
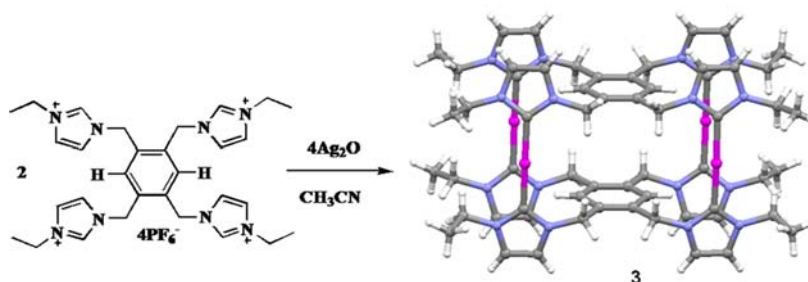
ASSOCIATED CONTENT

S **Supporting Information**

Characterization data and crystallographic information file. This material is available free of charge via the Internet at http://pubs.acs.org.

AUTHOR INFORMATION

Corresponding Author
*E-mail: icpg@iacs.res.in.

Present Address
†Institute of Condensed Matter and Nanosciences (IMCN) Bio- and Soft Matter (BSMA), Université catholique de Louvain, Louvain-la-Neuve 1348, Belgium.

Notes
The authors declare no competing financial interest.

ACKNOWLEDGMENTS

REFERENCES

(1) (a) Lehn, J.-M. *Supramolecular Chemistry: Concepts and Perspectives*; VCH: Weinheim, Germany, 1995. (b) *Frontiers in Supramolecular Chemistry*; Schneider, H., Dürr, H., Eds.; VCH: Weinheim, Germany, 1991. (c) *Comprehensive Supramolecular Chemistry*; Lehn, J.-M., Atwood, J. L., Davis, J. E. D., MacNicol, D. D., Vögtle, F., Eds.; Pergamon: Oxford, U.K., 1987−1996; Vols. *1−11*. (d) Yeh, R. M.; Davis, A. V.; Raymond, K. N. *Comprehensive Coordination Chemistry II*; McCleverty, J. A., Meyer, T. J., Eds.; Elsevier: Oxford, U.K., 2004; Vol. 7, pp 327−355. (e) Schalley, C. A.; Beizai, K.; Vögtle, F. *Acc. Chem. Res.* **2001**, *34*, 465−476. (f) De, S.; Mahata, K.; Schmittel, M. *Chem. Soc. Rev.* **2010**, *39*, 1555−1575. (g) Chakrabarty, R.; Mukherjee, P. S.; Stang, P. J. *Chem. Rev.* **2011**, *111*, 6810−6918. (h) Amouri, H.; Desmarets, C.; Moussa, J. *Chem. Rev.* **2012**, *112*, 2015−2041. (i) Koblenz, T. S.; Wassenaar, J.; Reek, J. N. H. *Chem. Soc. Rev.* **2008**, *37*, 247−262. (j) Furutani, Y.; Kandori, H.; Kawano, M.; Nakabayashi, K.; Yoshizawa, M.; Fujita, M. *J. Am. Chem. Soc.* **2009**, *131*, 4764−4768. (k) Mastalerz, M.; Oppel, I. M. *Angew. Chem., Int. Ed.* **2012**, *51*, 5252−5255. (l) Meng, W.; Breiner, B.; Rissanen, K.; Thoburn, J. D.; Clegg, J. K.; Nitschke, J. R. *Angew. Chem., Int. Ed.* **2011**, *50*, 3479−3483. (m) Brusilowskij, B.; Neubacher, S.; Schalley, C. A. *Chem. Commun.* **2009**, 785−787. (n) Kreickmann, T.; Hahn, F. E. *Chem. Commun.* **2007**, 1111−1120.

(2) (a) Brinker, U. H.; Mieusset, J.-L. *Molecular Encapsulation: Organic Reactions in Constrained Systems*; John Wiley & Sons: Chichester, U.K., 2010. (b) *Monographs in Supramolecular Chemistry*; Stoddart, J. F., Ed.; Royal Society of Chemistry: Cambridge, U.K., 1989 and 1991; Vols. *1−6*, pp 1994−1996. (c) Lindoy, L. F.; Atkinson, I. M. *Self-Assembly in Supramolecular Systems*; Royal Society of Chemistry: Cambridge, U.K., 2000. (d) Sun, Q.-F.; Iwasa, J.; Ogawa, D.; Ishido, Y.; Sato, S.; Ozeki, T.; Sei, Y.; Yamaguchi, K.; Fujita, M. *Science* **2010**, *328*, 1144−1147. (e) Klosterman, K.; Yamauchi, Y.; Fujita, M. *Chem. Soc. Rev.* **2009**, *38*, 1714−1725. (f) Jiang, W.; Schalley, C. A. *Proc. Natl. Acad. Sci. U.S.A.* **2009**, *106*, 10425−10429. (g) Brusilowskij, B.; Dzyuba, E. V.; Troff, R.; Schalley, C. A. *Chem. Commun.* **2011**, *47*, 1830−1832. (h) Bar, A. K.; Chakrabarty, R.; Mostafa, G.; Mukherjee, P. S. *Angew. Chem., Int. Ed.* **2008**, *47*, 8455−8459. (i) Zhao, Z.; Zheng, Y.-R.; Wang, M.; Pollock, J. B.; Stang, P. J.

Inorg. Chem. **2010**, *49*, 8653−8655. (j) Smulders, M. M. J.; Jiménez, A.; Nitschke, J. R. *Angew. Chem., Int. Ed.* **2012**, *51*, 6681−6685. (k) Wang, M.; Zheng, Y.-R.; Ghosh, K.; Stang, P. J. *J. Am. Chem. Soc.* **2010**, *132*, 6282−6283. (l) Zheng, Y.-R.; Lan, W.-J.; Wang, M.; Cook, T. R.; Stang, P. J. *J. Am. Chem. Soc.* **2011**, *133*, 17045−17055. (m) Banerjee, M.; Das, S.; Yoon, M.; Choi, H. J.; Hun, M. H.; Park, S. M.; Seo, G.; Kim, K. *J. Am. Chem. Soc.* **2009**, *131*, 7524−7525. (n) Samanta, D.; Shanmugaraju, S.; Joshi, S. A.; Patil, Y. P.; Nethaji, M.; Mukherjee, P. S. *Chem. Commun.* **2012**, *48*, 2298−2300. (o) Ficks, A.; Sibbald, C.; John, M.; Dechert, S.; Meyer, F. *Organometallics* **2010**, *29*, 1117−1126. (p) Smulders, M. M. J.; Riddell, I. A.; Browne, C.; Nitschke, J. R. *Chem. Soc. Rev.* **2013**, *42*, 1728−1754.

(3) (a) Hamilton, A. D. *Supramolecular Control of Structure and Reactivity: Perspectives in Supramolecular Chemistry*; John Wiley & Sons: Oxford, U.K., 1996; Vol. 3. (b) Chambron, J.-C.; Dietrich-Buchecker, C.; Sauvage, J.-P. Transition Metals as Assembling and Templating Species. In *Comprehensive Supramolecular Chemistry*; Lehn, J.-M., Atwood, J. L., Davis, J. E. D., MacNicol, D. D., Vögtle, F., Eds.; Pergamon Press: Oxford, U.K., 1996; Vol. 9, Chapter 2, p 43. (c) Chen, C.-L.; Zhang, J.-Y.; Su, C.-Y. *Eur. J. Inorg. Chem.* **2007**, 2997−3010. (d) Shanmugaraju, S.; Vajpayee, V.; Lee, S.; Chi, K.-W.; Stang, P. J.; Mukherjee, P. S. *Inorg. Chem.* **2012**, *51*, 481−4823. (e) Meng, W.; Clegg, J. K.; Nitschke, J. R. *Angew. Chem., Int. Ed.* **2012**, *51*, 1881−1884. (f) Bilbeisi, R. A.; Clegg, J. K.; Elgrishi, N.; Hatten, X.; Devillard, M.; Breiner, B.; Mal, P.; Nitschke, J. R. *J. Am. Chem. Soc.* **2012**, *134*, 5110−5119. (g) Bar, A. K.; Chakrabarty, R.; Mukherjee, P. S. *Inorg. Chem.* **2009**, *48*, 10880−10882. (h) Meng, W.; Clegg, J. K.; Thoburn, J. D.; Nitschke, J. R. *J. Am. Chem. Soc.* **2011**, *133*, 13652−13660. (i) Fan, J.; Saha, M. L.; Song, B.; Schönherr, H.; Schmittel, M. *J. Am. Chem. Soc.* **2012**, *134*, 150−153. (j) Kilbas, B.; Mirtschin, S.; Scopelliti, R.; Severin, K. *Chem. Sci.* **2012**, *3*, 701−704. (k) Zysman-Colman, E.; Denis, C. *Coord. Chem. Rev.* **2012**, *256*, 1742−1761. (l) Birkmann, B.; Ehlers, A. W.; Fröhlich, R.; Lammertsma, K.; Hahn, F. E. *Chem.—Eur. J.* **2009**, *15*, 4301−4311.

(4) (a) Rit, A.; Pape, T.; Hahn, F. E. *J. Am. Chem. Soc.* **2010**, *132*, 4572−4573. (b) Rit, A.; Pape, T.; Hepp, A.; Hahn, F. E. *Organometallics* **2011**, *30*, 334−347. (c) Hahn, F. E.; Radloff, C.; Pape, T.; Hepp, A. *Organometallics* **2008**, *27*, 6408−6410. (d) Radloff, C.; Hahn, F. E.; Pape, T.; Fröhlich, R. *Dalton Trans.* **2009**, 7215−7222. (e) Radloff, C.; Weigand, J. J.; Hahn, F. E. *Dalton Trans.* **2009**, 9392−9394. (f) Conrady, F. M.; Fröhlich, R.; Schulte to Brinke, C.; Hahn, F. E. *J. Am. Chem. Soc.* **2011**, *133*, 11496−11499. (g) Schmidtendorf, M.; Pape, T.; Hahn, F. E. *Angew. Chem., Int. Ed.* **2012**, *51*, 2195−2198. (h) Lin, I. J. B.; Vasam, C. S. *Coord. Chem. Rev.* **2007**, *251*, 642−670. (i) Radloff, C.; Gong, H.-Y.; Schulte to Brinke, C.; Pape, T.; Lynch, V. M.; Sessler, J. L.; Hahn, F. E. *Chem.—Eur. J.* **2010**, *16*, 13077−13081.

(5) (a) Ustinov, A.; Weissman, H.; Shirman, E.; Pinkas, I.; Zuo, X.; Rybtchinski, B. *J. Am. Chem. Soc.* **2011**, *133*, 16201−16211. (b) Mahata, K.; Schmittel, M. *J. Am. Chem. Soc.* **2009**, *131*, 16544−16554. (c) Vajpayee, V.; Song, Y. H.; Cook, T. R.; Kim, H.; Lee, Y.; Stang, P. J.; Chi, K.-W. *J. Am. Chem. Soc.* **2011**, *133*, 19646−19649.

(6) (a) Su, C.-Y.; Cai, Y.-P.; Chen, C.-L.; Smith, M. D.; Kaim, W.; Loye, H.-C. *J. Am. Chem. Soc.* **2003**, *125*, 8595−8613. (b) Hartshorn, C. M.; Steel, P. J. *Inorg. Chem. Commun.* **2000**, *3*, 476−481. (c) Su, C.-Y.; Cai, Y.-P.; Chen, C.-L.; Lissner, F.; Kang, B.-S.; Kaim, W. *Angew. Chem., Int. Ed.* **2002**, *41*, 3371−3375. (d) Caulder, D. L.; Powers, R. E.; Parac, T. N.; Raymond, K. N. *Angew. Chem., Int. Ed.* **1998**, *37*, 1840−1843. (e) Müller, I. M.; Möller, D.; Schalley, C. A. *Angew. Chem., Int. Ed.* **2005**, *44*, 480−484. (f) Maurizot, V.; Yoshizawa, M.; Kawano, M.; Fujita, M. *Dalton Trans.* **2006**, 2750−2756. (g) Steel, P. J.; Sumby, C. J. *Chem. Commun.* **2002**, 322−323. (h) Kumazawa, K.; Yamanoi, Y.; Yoshizawa, M.; Kusukawa, T.; Fujita, M. *Angew. Chem., Int. Ed.* **2004**, *43*, 5936−5940. (i) Hahn, F. E.; Radloff, C.; Pape, T.; Hepp, A. *Chem.—Eur. J.* **2008**, *14*, 10900−10904. (j) Ahamed, B. N.; Arunachalam, M.; Ghosh, P. *Inorg. Chem.* **2011**, *50*, 4772−4780. (k) Wang, M.; Lan, W.-J.; Zheng, Y.-R.; Cook, T. R.; White, H. S.; Stang, P. J. *J. Am. Chem. Soc.* **2011**, *133*, 10752−10755.

(7) Su, C.-Y.; Cai, Y.-P.; Chen, C.-L.; Zhang, H.-X.; Kang, B.-S. *J. Chem. Soc., Dalton Trans.* **2001**, 359−361.

(8) (a) Hahn, F. E.; Jahnke, M. C. *Angew. Chem., Int. Ed.* **2008**, *47*, 3122−3172. (b) Raynal, M.; Cazin, C.S. J.; Vallée, C.; Olivier-Bourbigou, H.; Braunstein, P. *Dalton Trans.* **2009**, 3824−3832.

(9) (a) *SAINT and XPREP*, 5.1 ed.; Siemens Industrial Automation Inc.: Madison, WI, 1995. Sheldrick, G. M. (b) *SADABS, Empirical Absorption Correction Program*; University of Göttingen: Göttingen, Germany, 1997.

(10) Sheldrick, G. M. *SHELXTL Reference Manual*, version 5.1; Bruker AXS: Madison, WI, 1997.

(11) Sheldrick, G. M. *SHELXL-97: Program for Crystal Structure Refinement*; University of Göttingen: Göttingen, Germany, 1997.

(12) Spek, A. L. *PLATON-97*; University of Utrecht: Utrecht, The Netherlands, 1997.

(13) *Mercury 2.3 supplied with Cambridge Structural Database*; CCDC: Cambridge, U.K..

(14) (a) Liu, X.; Pattacini, R.; Deglmann, P.; Braunstein, P. *Organometallics* **2011**, *30*, 3302−3310. (b) Stępień, M.; Latos-Grażyński, L. *J. Am. Chem. Soc.* **2002**, *124*, 3838−3839. (c) Munakata, M.; Wu, L. P.; Ning, G. L. *Coord. Chem. Rev.* **2000**, *198*, 171−203.